Study of the I–V Characteristics of Organic Light-Emitting Diodes Based on Thiophene Vynilic Derivatives

F. Brovelli,[1] J. C. Bernède,[2] S. Marsillac,[2] F. R. Díaz,[1] M. A. Del Valle,[1] C. Beaudouin[2]

[1]*Facultad de Química, Pontificia Universidad Católica de Chile, Vicuña Mackenna 4860, Casilla 306, Correo 22, Santiago, Chile*
[2]*EPSE-Facultè des Sciences et des Techniques de Nantes, 2 rue de Houssinière, BP 92208, F-44322 Nantes Cedex 3, France*

Received 26 June 2001; accepted 17 January 2002

ABSTRACT: Organic light-emitting diodes were obtained using a thiophene vynilic derivative polymer electrochemically synthesized. The electrochemistry of the thiophene vynilic derivative, 1,5-*bis*(2-thienyl)-1,4-pentadien-3 one (CDV), was conducted in a nonaqueous media. The polymer was deposited on tin oxide (SnO_2)-coated glass substrates. The films obtained were physicochemically characterized by infrared absorption, a scanning microscope, microprobe X-ray photoelectron analysis, and photoluminescence measurements. It was shown that the coverage efficiency of the films is very high. There is some oxygen contamination, not only at the surface, but also in the bulk of the polymers. The films are photoluminescent with emission between 660 and 720 nm. The current–voltage (I–V) characteristics exhibit a turn-on voltage at about 2–4 V depending on the film thickness (120–250 nm). The electroluminescence–voltage (EL–V) curve has a similar shape but a shift of 1–2 V toward higher voltage. In the conducting state, there is no significant dependence of the temperature upon the current. All these facts cannot be explained easily by a simple thermionic model; a thermally activated tunneling effect appears more adequate. The current in the small potential domains has a behavior more or less erratic with a differential negative resistance and a switching effect. This behavior, arising from localized pathways, has a nature different from the injection processes, allowing electroluminescence. These pathways are related to surface heterogeneities (SnO_2/polymer films) and aluminum diffusion. By not being directly related to electroluminescence, these pathways could induce a heating effect and an irreversible short-circuit effect. © 2002 Wiley Periodicals, Inc. J Appl Polym Sci 86: 1128–1137, 2002

Key words: diodes; electrochemistry; ESCA/XPS; luminescence

INTRODUCTION

Since the first report of electroluminescence from organic conjugate polymers,[1] effort has been devoted to the design of light-emitting devices. Organic light-emitting diodes (OLEDs) are composed of three or more layers.[2] The first one is a transparent conductive oxide (TCO). The second layer is an organic active film, which can be a multilayer, in order to improve the electroluminescence efficiency.[2–7] The third layer is, most of the time, an Al film because of its relatively low work function and its good stability compared to that of metal with a lower work function such as Ca.

Here, we report on an investigation of the charge carrier injection mechanism of electrochemically synthesized polymers. We concentrated mainly on a discussion of the current–voltage (I–V) curves measured for different thicknesses of the polymer and for different temperatures. For the active layer, we used a polymer based on a thiophene vynilic derivative (Scheme 1). Polymers with thiophene units have often been used in OLEDs.[8] The modification of the properties of these structures with different lateral chain substitution on the thiophene nucleus have been studied. It has been shown that the transport properties, the emitted light color, and the stability of the devices can be monitored by such a process.

In the present work, we proceeded to a central thiophene nucleus substitution, that is, to the incorporation of an organic function in the 2–2′ position. The organic function used was 1,4-pentadien-3-one. Our purpose was to study the effect of such organic functions on the optoelectrical properties of the polymers after substitution in the polymer chains. The main characteristic of this substituted product is that it has π electrons, which induce a limited electronic delocalization to the new polymers. Such limited delocalization should decrease the carrier leakage toward electrodes. Moreover, the effect of the chain modifications introduced here should be an increase of the band gap, that is, a blue-shift effect on the emission spectrum of the polymers.

Correspondence to: J. C. Bernède (jean-christian.bernede@physique.univ-nantes.fr).

Contract grant sponsor: FONDECYT-CHILE; contract grant number: 8970011.
Contract grant sponsor: ECOS-CONICYT; contract grant number: C99E05.

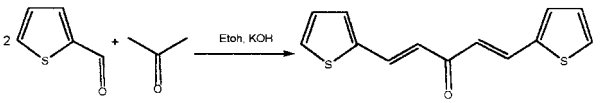

Scheme 1

The TCO and metallic films are deposited by evaporation under a vacuum. Usually, the organic film is deposited by spin-coating. However, other techniques such as electrochemistry can be used, but it has been rarely been used up to now[9,10] because of the high processability of spin-coating. On the other hand, electrochemical polymerization presents interesting advantages such as

- Direct deposition of the polymer onto the TCO substrate;
- Formation of a film with good adhesion and mechanical properties; and
- Possibility of controlling different parameters during the polymerization by varying parameters such as the concentration of the starting material, the solvent–salt combination, as well as electrochemical ones.

All this makes possible the tailoring of the final polymer film material into a certain structure and morphology.

EXPERIMENTAL

Monomer synthesis

1,5-Bis[2-thienyl]-1,4-pentadien-3one, abbreviated CDV, was synthesized according to ref. 7, following Scheme 1. Orange crystals were obtained.

Mp, 113–114°C.^{1}H-NMR (200 MHz, $CDCl_3$): δ = 7.86 (1H,d), 7.42 (1H,d), 7.35 (1H,d), 7.09 (1H,dd), 6.83 (1H,d).

Anal. Found: C, 62.81%; H, 4.08%; S, 24.51%.

Electrochemical setup

The TCO used was commercial SnO_2 (Solems, Palaiseau, France). The whole glass substrate was fully covered; therefore, some SnO_2 had to be removed. After masking a line 2 mm broad, the SnO_2 was etched using Zn + HCl as an etchant.[11] Then, the substrates were cleaned using a H_2O_2 treatment following a process described by Osada et al., [12] which corresponds to the first solution (SC1) of the RCA process first described by Kern and Puotinen.[13] The substrates were treated with an 80°C H_2O—H_2O_2 (30%)—NH_4OH (25%) solution (5:1:1 volume parts) for 20 min, followed by rinsing with boiling distilled water for 5 min. The use of boiling water has been proved to be helpful in obtaining clean surfaces.[14]

The setup for cyclic voltammetry was described previously.[15] A SnO_2 electrode (geometrical area 0.4 cm^2) and Ag/AgCl in a tetramethylammoniun chloride solution (Me_4NCl)[16] were used as working and reference electrodes, respectively. The so-measured potentials were referred to those of the saturated calomel electrode (SCE). A stainless-steel AISI 316 gauze, separated from the working electrode compartment by a frie glass frit, was used as a counterelectrode. Prior to all the experiments, solutions were purged with high-purity argon and an argon atmosphere was maintained over the solution during the measurements. Acetonitrile (Aldrich, anhydrous) was stored in an atmosphere of dry argon and over molecular sieves (4 Å). To achieve a minimum water content, the solvents were manipulated with syringes. The supporting electrolyte was tetrabutylammonium tetrafluorborate (Bu_4NBF_4) supplied by Aldrich (France) and was dried under a vacuum at 60°C. The electrochemical polymerization of CDV was carried out from solutions containing 0.025*M* of the monomer and 0.1*M* Bu_4NBF_4. Polymerization was achieved by cycling between −0.5 to 2.5 V versus the SCE at 8.3 mV/s.

Characterization techniques

The films were first characterized by infrared absorption (IR). IR spectra were obtained with an FTIR spectrometer. Absorption band positions are given in wavenumbers (cm^{-1}). To measure the CDV films, they were scratched out from the substrate and then mixed with some KBr powder. Thin pellets of the mixture were pressed just before the measurement.

Observation of the surface morphology of the surface and of the cross section of the layers was performed using a JEOL 6400F field-effect scanning electron microscope (SEM) to compare the surface topography of the PBrPDSe and of the CZ and to check the cross section. Electron probe microanalysis (EPMA) was used for qualitative analysis.

Electron spectroscopy for chemical analysis (ESCA) measurements were conducted with a Leybold spectrometer at the University of Nantes CNRS. The ESCA was used for XPS measurements. The X-ray source was a magnesium cathode (1253.6 eV) operating at 10 kV and 10 mA. The energy resolution was 1 eV at a pass energy of 50 eV. High-resolution scans with a good signal/noise ratio were obtained in the C1*s*, S2*p*, O1*s*, and N1*s* regions of the spectrum. The quantitative studies were based on the determination of the C1*s*, S2*p*, O1*s*, and N1*s* peaks areas: 0.2, 0.44, 0.6 and 0.36, respectively, as sensitive factors; the sensitivity factors were given by the manufacturer. The vacuum in the analysis chamber was about 10^{-6} Pa. All the spectra were recorded under identical conditions.

The decomposition of the XPS peaks into different components and the quantitative interpretation were

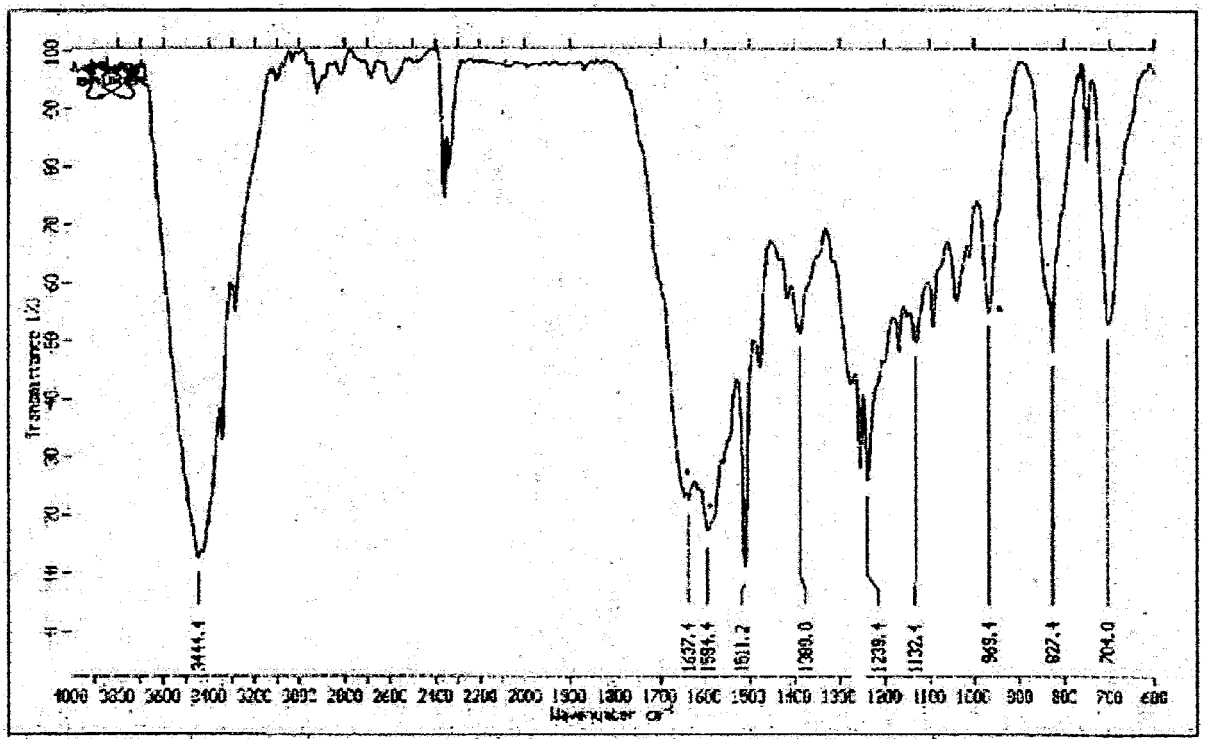

Figure 1 IR absorption spectra of CDV.

made after the subtraction of the background using the Shirley method.[17] The developed curve-fitting programs permit the variation of parameters, such as the Gaussian/Lorentzian ratio, the full width at half-maximum (fwhm), and the position and the intensity of the contributions. These parameters were optimized by the curve-fitting program to obtain the best fit.

The photoluminescence (PL) spectra were recorded using a Jobin–Yvon TG HG2S spectrophotometer with holographic gratings. The signal was detected with a Peltier-cooled photomultiplier. The sample was excited with the 337-nm line of a filtered xenon lamp (150 W). The laser power for the sample was kept below 2 mW. Experiments were performed at room temperature.

Light-emitting diodes (LEDs) were prepared by deposition of Al under a vacuum on top of the polymeric film deposited onto a SnO_2-coated glass substrate. The deposition rate was 1 ns^{-1}, and the film thickness was about 300 nm. During aluminum deposition, the substrate holder was cooled by a liquid nitrogen flow. The I–V curves were measured by a Keithley 617 programmable electrometer, a Keithley 2000 multimeter, and a Lambda IEEE-488 programmable power supply Model LLS6060-GPIB interfaced to an IBM PC computer.

Electroluminescene (EL) was detected through the transparent SnO_2 electrode and glass. The light output was detected using a silicon photodiode and a Keithley 617 electrometer.

RESULTS

Before characterization of the device, we carried out a physicochemical characterization of the polymer: MEB, EPMA, and XPS.

Physicochemical characterization

A typical IR spectrum of a CDV film is presented Figure 1, while the main absorption bands are given in Table I. It can be seen that the presence of typical bonds, such as C═O and C—S, clearly testifies that CDV was deposited onto the substrates.

The visualization of the films has shown that there is a high coverage efficiency of the deposition process

TABLE I
Attribution of the Main IR Absorption Bands

Wavenumber (cm^{-1})	Attribution
3444	O—H
1637	C═C
1594	C═O + O—H
1511	C═C (cycle)
1389	C—C (cycle)
1236	C—S
1042	C—H (cycle)
969	C═C (cycle)
827, 704	C—H outside of the cycle plane (substituant 2 and 2,5)

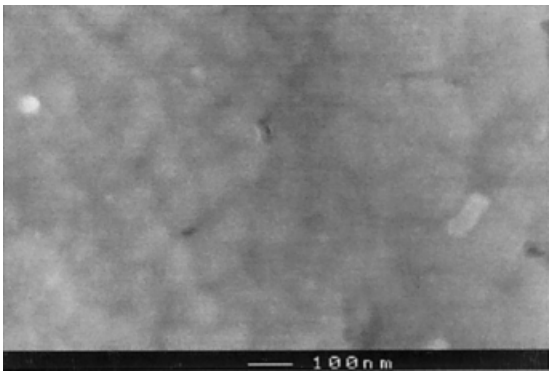

Figure 2 Microphotograph of a CDV thin film (thickness 150 nm).

(Fig. 2). No pinholes are visible after five voltammetric cycles. We checked, in the back-scattering electron mode, that the composition is homogeneous, as shown by the uniform color of the images (not shown).

The composition was estimated by EPMA. In each case, there is some oxygen contamination and also some nitrogen is present (Table II). These extra atoms can be related to air, electrolyte salt, and/or solvent contamination. This was checked by XPS measurements. The XPS quantitative analysis confirmed the contamination by oxygen while some nitrogen also was found (Table II). XPS, being a surface analysis, measures mainly surface contamination. However, the large oxygen excess measured is in good agreement with the EPMA study. Also, there is some relative sulfur deficiency, confirming film contamination.

In some samples, small amounts of the dopant (fluorine) are present. However, often, the atomic dopant relative concentrations of the dopant are small and the doping process can be considered as reversible. This undoping possibility is very important for OLED application since it has been shown that, usually, the PL effect decreases in the presence of dopant counterions. Therefore, only dedoped samples were used for the luminescence experiment.

It should be noted that the etching speed of oxygen and nitrogen is far higher than that of carbon. Therefore, during etching, the C—N and C—O bonds are preferentially broken and no real information about the polymer can be obtained after such a process.

We proceeded to a decomposition of the XPS peaks (Fig. 3). Some nitrogen superficial contamination is noted in this polymer, while sulfur deficiency and oxygen excess are also observed (Table II). No dopant was detected by XPS.

The decomposition of the C1*s* peak [Fig. 3(a)] shows that four contributions are necessary to obtain a good fit between the experimental and theoretical curves. The first contribution, situated at 285 eV, can be attributed to the C—C bond. This C—C binding energy was taken as a reference, as is often the case.[18] The second one at 286 eV is more difficult to attribute. Its binding energy is a little too high to be attributed to C—S, but it is a little too small to be attributed to C—OH. In fact, it corresponds to C—N. However, the relative atomic value of the contribution (23 at %) cannot be attributed to C—N contamination only; therefore, it should be attributed to a mixture of C—S, C—N, and C—OH. There is a possibility of the fitting program being too limited to obtain more information.

The third contribution situated at 287.5 eV corresponds to the expected C═O bonds and may also be due to a surface contamination contribution. The fourth peaks can be assigned to COOH surface contamination.

The O1*s* peak [Fig. 3(b)] can be split into two contributions: The first one, situated at about 533 eV, corresponds to the C═O bonds of the polymer; the second one, at 533.4, can be assigned to contamination. It may correspond to some C—OH contaminant, but also to some absorbed H_2O.[19]

It is worth noting that the S2*p* line corresponds to a doublet. However, it can be seen in Figure 3(c) that more than a doublet is needed to obtain a good decomposition of the peak. The main contribution, at 164.3 eV, corresponds to C—S bonds of the polymer. The small contribution at 168.5 eV corresponds to oxidized sulfur, due to some superficial sulfur oxidation. The small nitrogen contribution [Fig. 3(d)] corresponds to covalent nitrogen, which can be assigned to air contamination but also to some solvent contribution, since some nitrogen is also present in the bulk of the films as shown by EPMA. It was observed that, after an etching of 1 min, in the case of sulfur, only the contribution corresponding to the C—S bonds is still present, showing that the S oxidation occurs at the surface.

A typical photoluminescent measurement is shown in Figure 4. It can be seen that emission is recorded between 660 and 720 nm with a maximum at about 680 nm, which corresponds to an emission of orange light.

I–V and EL–V experimental results

The forward direction corresponds to a positive bias on the SnO_2 electrode. The electrical behavior of di-

TABLE II
CDV Quantitative Analysis

	Sample			
	C	O	S	N
Analysis	At %			
Theoretical	81.25	6.25	12.5	0
EPMA	78	12	8	2
XPS	66.5	24	5.5	4

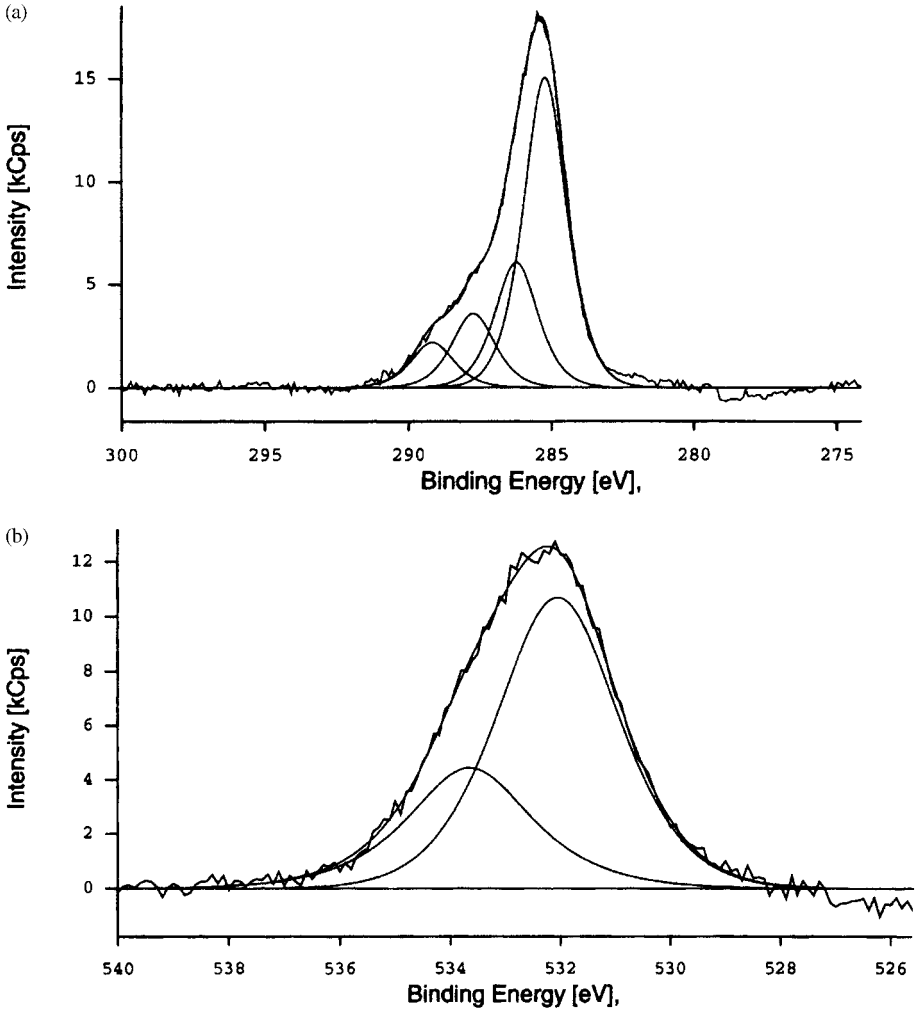

Figure 3 CDV 113: XPS peak decomposition: (a) C1*s*; (b) O1*s*; (c) S2*p*; (d) N1s; (〰) experimental results; (—) theoretical curve; (—) different components.

odes measured at room conditions under forward bias follows a characteristic diode behavior (Fig. 5). This figure also shows the EL–V characteristic. We note that the turn-on voltage value is quite small. The luminescence appears after the turn-on voltage, that is, the EL turn-on voltage is 1–2 V higher than is the electric turn-on voltage. It can be seen that, on slowly increasing the applied bias to a new diode, the behavior is first ohmic for low voltage, but the current varies widely between devices. When the potential increases, the current often becomes noisy in the range 0.2–2.0 V. Often, the current becomes superlinear and then switches off. In that domain, the current may vary by several orders of magnitude between devices and more than one switching can be put into evidence (Fig. 6). When the turn-on voltage is achieved, the noise disappears and the current increases exponentially with the voltage (Fig. 5). As described above, following this current increase, the EL emission appears and increases with the current. In the reverse direction, a similar switching effect is present in the small-voltage domain; however, application of higher voltage, even for short periods, appears to be more damaging than is the same forward bias.

The effect of the thickness of the organic layer on the I–V curves was studied (Fig. 7). The thickness of the films was varied with the number of voltammetric cycles. The thickness of the films was measured by interferometry. The measured thickness varies between 125 and 250 nm. It can be seen that there is no significant dependence of the temperature on the current.

The variation of the current, in the conductive state of the diode (V = 3.5 V), with the temperature is reported Figure 8. It can be seen that this variation is very small.

DISCUSSION

The experimental physicochemical characterization showed that the deposited films exhibit the typical IR absorption bands expected for the polymer electropo-

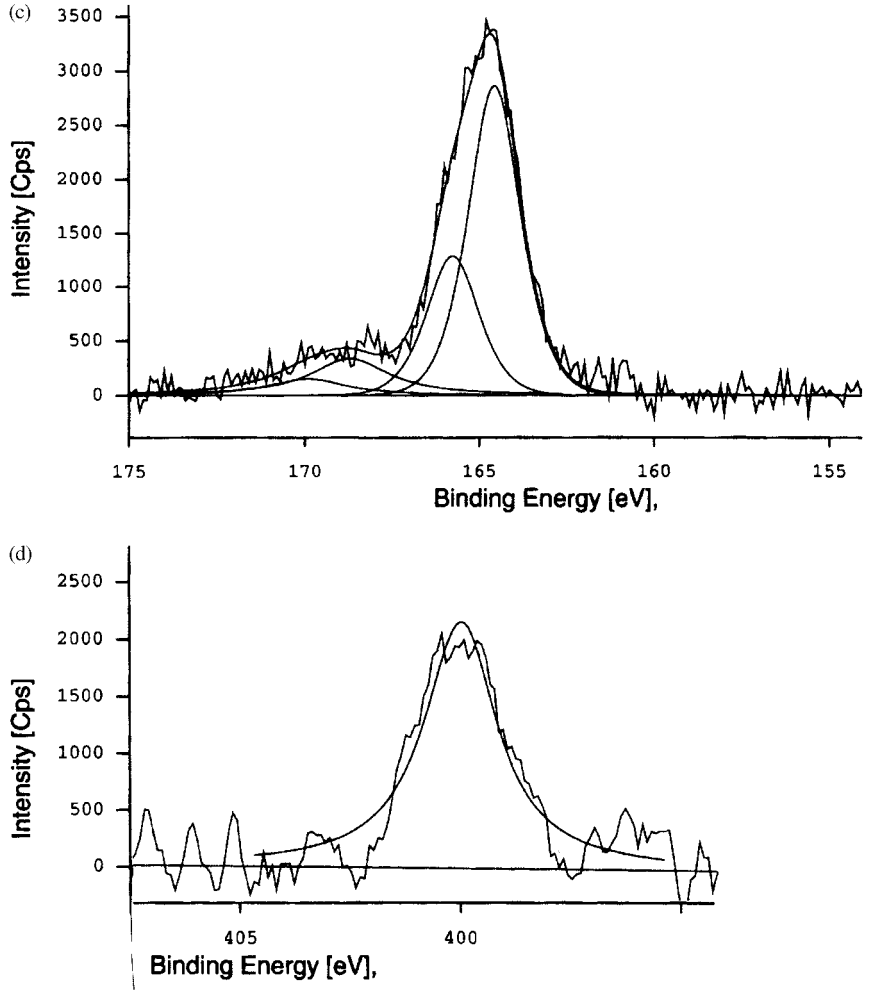

Figure 3 (*Continued*)

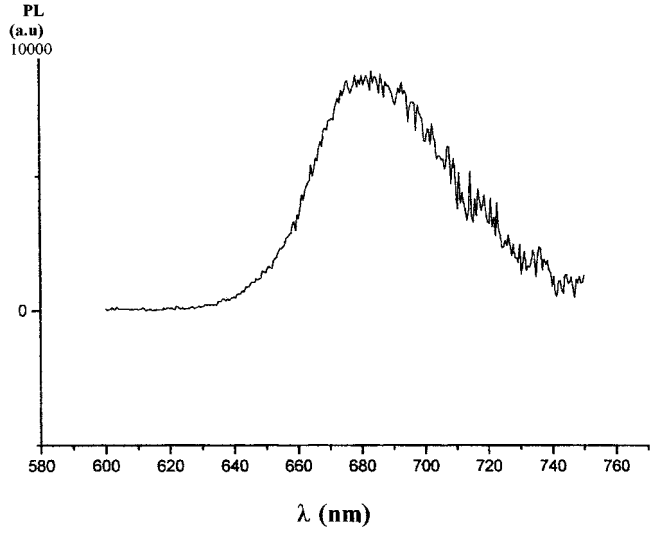

Figure 4 Photoluminescence spectra of CDV film electrochemically synthesized.

lymerized (Table I and Fig. 1). After five cycles, the samples are pinhole free. The films present a good adherence to the substrate. They are surface-contaminated; also, there is some oxygen contamination of the films. Probably, some trace of water (moisture) is present in the bulk of the films. The films, which are dedoped at the end of the process, have been used to grow OLEDs. As shown Figure 4, the CDV films are luminescent between 660 and 720 nm.

The understanding of the electrical process appears very important in achieving highly performing diodes. It was shown that, in the current voltage (I–V) characteristics, the dominant conduction mechanism cannot be either ohmic, trap-free-space charge limited or purely tunneling injection. The temperature and thickness dependence indicate that it must be either thermionic emission or thermally assisted tunneling.[20] In the present article, experimental results are discussed with the help of these previous studies.

To interpret the I–V characteristics, the structure can be assimilated to an M/SCp (metal/p-type semiconductor) contact, M being SnO_2, and SCp, the polymer

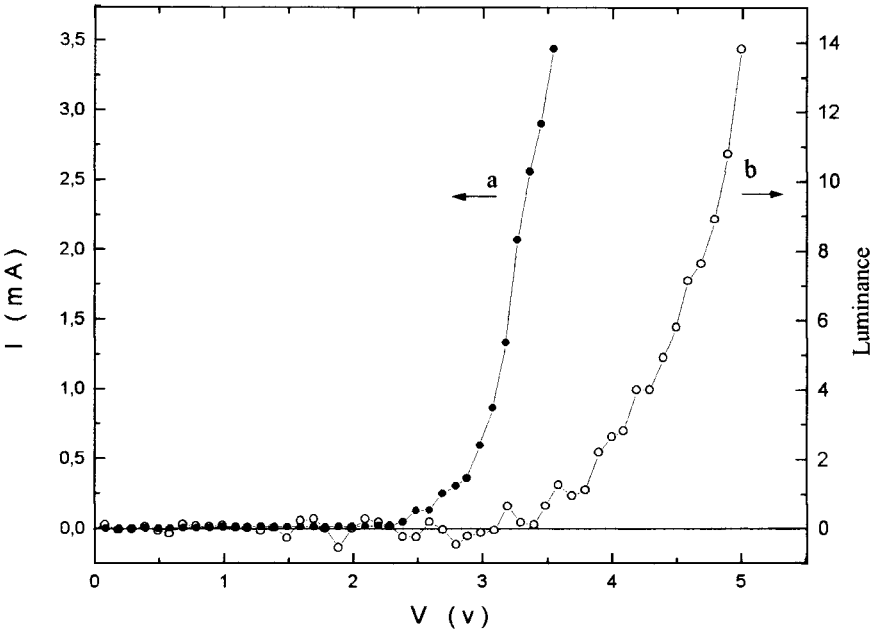

Figure 5 (a) Typical I–V curve and (b) corresponding EL–V, the CDV being electrochemically synthesized.

which is a hole-transport layer (HTL). In that case, the thermionic emission theory gives[21]:

$$J = J_{st}\left[\exp\left(\frac{qV}{nkT}\right) - 1\right] \tag{1}$$

where

$$J_{st} = A^*T2\exp\left(\frac{q\phi_B}{kT}\right)$$

with A^* the Richardson constant; ϕ_B, the barrier height; and n, an ideality factor.

It can be seen in Figure 9 that a good fit can be obtained in the turn-on voltage range. However, values of 10–40 are found for the ideality factor n (Table III) by these fits, indicating that the model of a standard Schottky contact, for which values of n = 1–2 are typical,[21] is not applicable here. Moreover, the variation of the turn-on voltage with the thickness corroborates that a simple thermionic model cannot be used in the present work. Even if series resistances can justify higher values of n than 2 and thickness dependence, it cannot justify the very small dependence on the temperature.

In Figure 8, we report, with the experimental results (dotted line), the theoretical variation which should be obtained with a barrier height of 0.2 eV, the barrier height value deduced from Figure 9 with A^* = 120 A cm^{-2} K^{-2}. It can be seen that the simple thermionic model definitely cannot be used to explain the I–V characteristics.

The CDV polymer, as other thiophene derivatives, is an HTL and, therefore, it has been shown that the current is mainly a hole current.[8] Therefore, the I–V characteristics can be attributed to a hole-only device. Since the SnO_2/CDV/Al structure shows only a slight temperature dependence rather than the exponential dependence expected for thermionic emission, the field-dependent behavior of the characteristics will be associated with the tunneling process. The tunneling process is well described by the Fowler–Nordheim theory[22]:

$$I\alpha F^2\exp\left(\frac{-K}{F}\right) \tag{2}$$

where F is the electric field and

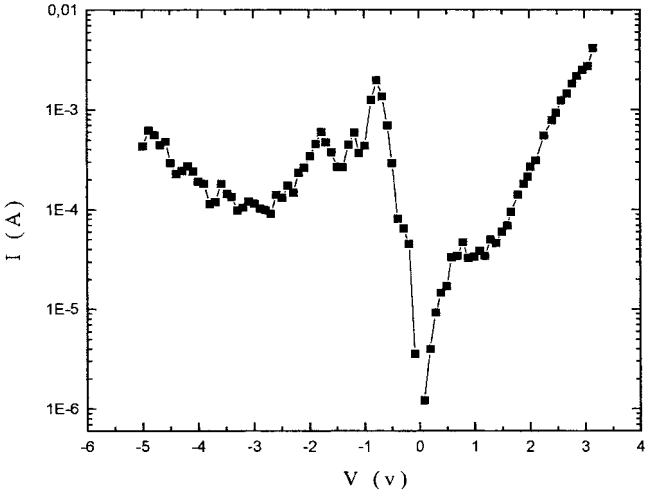

Figure 6 Erratic behavior of the current for small potential.

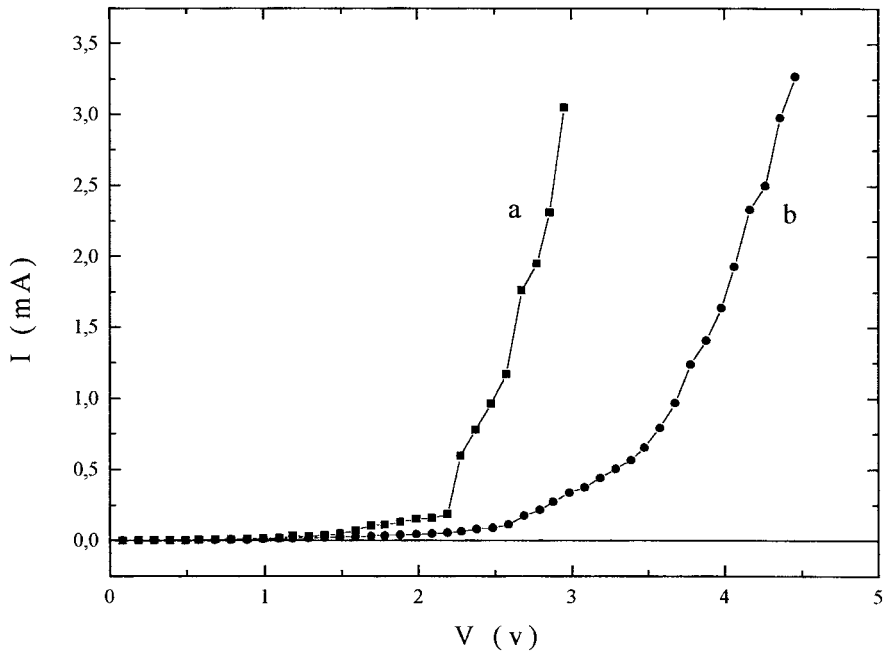

Figure 7 Evolution of the turn-on voltage with the CDV polymer film thickness: (a) thickness 120 nm; (b) thickness 250 nm.

$$K = \frac{8\pi\sqrt{2m^*}\varphi^{3/2}}{3qh}$$

φ is the barrier height and m^* is the effective mass of the holes in the polymer.

Assuming that the electric field is constant across the device and that the effective mass equals the free-electron mass, the barrier height can be estimated. Figure 10 shows a plot of $\ln(I/F^2)$ versus $1/F$ of a SnO_2/CDV/Al device with a 100-nm-thick polymer layer. As predicted by the theory, above the turn-on voltage, the plot is linear. Therefore, the barrier height was estimated as discussed above and the values are reported Table III. These data indicate a constant barrier height of 0.2–0.28 eV for all CVD devices whatever the thickness of the sample.

In the low potential range, the high current flow and switching effects cannot be satisfactorily explained by usual models for charge-carrier injection or/and transport. The surface of the SnO_2 film is "roughly pyramidal"-shaped.[23] It should be also be noted that, even if the samples are cooled with liquid nitrogen during aluminum deposition, some metal diffusion can take place. All these facts could induce some leakage paths. These paths can justify the large current

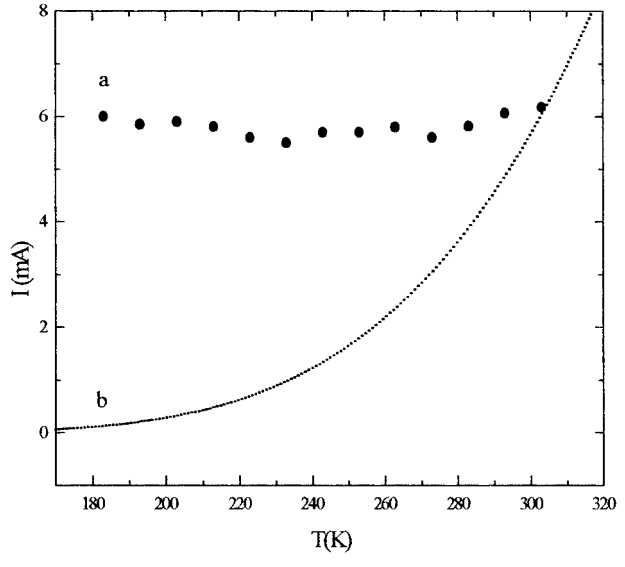

Figure 8 Temperature dependence of a SnO_2/CDV/Al structure operating at 3.5 V; for comparison, the solid line indicates the I–V characteristics of a 0.2-eV Schottky barrier device (b).

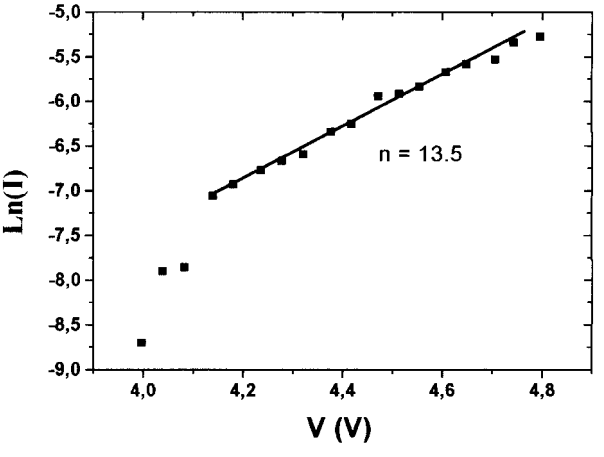

Figure 9 Semilogarithmic plots of I–V characteristics at a large forward bias for sample of Figure 4.

TABLE III
Ideality Factor *n* (Thermionic Model) and Barrier Height Φ (Fowler–Nordheim model) for Different OLEDs

	Structure SnO_2/CDV/A1: Sample					
Measurement	201	302	502	601	801	901
Ideality factor *n*	23	13	20	40	11	15
Barrier height (eV)	0.28	0.24	0.25	0.22	0.20	0.27

variation from one sample to another one for a small potential; in that case, the switching effect can be related to the burnout of these leakage paths.

The surface roughness of the SnO_2 film alone induces peaks to 50 nm. Therefore, models based on the homogeneity of the film and interface should be used very carefully. In the low-voltage domain, the maximum current value and the corresponding voltage can vary from one measurement to the next. Therefore, the negative differential resistance (NDR) measured can be reproduced only qualitatively. It can appear in both sweep directions. It should be noted that there is no EL in the voltage domain where NDR is present (Fig. 6). The current switching behavior independent of the EL measured can be explained by an equivalent circuit consisting of a conventional LED in parallel with an NDR.[24] The NDR takes place only at singular points, with current flowing though localized pathways. Since the EL is spatially homogeneous, it is not affected by this NDR. The localized pathways do not contribute to the EL.

The current flowing through localized pathways at low voltages has different properties compared to high voltages, so the transport mechanism of these pathways can be completely different. The reversibility, at least partially, of the NDR effect excludes simple burnout of shunts with increasing voltage. More probably, heterogeneities induce some preferential injection filament where processes similar to those described in amorphous chalcogenide switching devices[25,26] or metal/insulator/metal structures (MIM)[27] can take place.

Nevertheless, processes may take place related to the heating effect of the filament.[27] The erratic behavior of the current looks like that of MIM structures. For an alumina film thickness of about 100 nm and an aluminum electrode, Al/AlO_3/M structures exhibit NDR with an erratic current. Moreover, when the potential decreases, a similar NDR occurs but with smaller intensity, which has also been described in OLEDs.[24] The NDR in MIM structures was modeled by Deamaley et al.[28] The rough interface electrode/insulating film induces a very high electrical field localized on the tip heterogeneity at the interface. Such a high field induces conducting filament growth throughout the insulating films. This conducting filament growth corresponds to ionic migration thermally activated. These filaments are not considered to be perfectly uniform but to have weak spots, which determine their resistance and which become heated by the carrier flow. This induces hot spots in the filament and the conducting chain may be ruptured. This aspect will account for negative resistance and reversibility. The rupture of a filament will occur if T exceeds T_{max}. The filaments can reform subsequently, but this will depend on their temperature, the ambient temperature, the electronic field, and the possible space-charge effect.

A similar model based on the growth of conducting filaments through the organic insulating layer can presently be used. The filament initiation should take place at the interface roughness where very high electrical fields are localized. It has already be shown that switching on Al/BN/Si/Al can occur in the presence of humidity.[29] This switching behavior does bear a resemblance to NDR in our OLED structures. In a moist atmosphere, protons dissociated from the absorbed water migrate from the anode on the layer in the high electric field regions and form conductive filaments. Since it has been shown that some water is present in our structures, the same process can take place. After filament breakdown, with the roughness of the film not being modified, new filaments can grow again, which justify the erratic variation of the current but also the reversibility of the NDR effect. If such effects are fundamentally different from those related to EL, we cannot exclude that they can be active in the high-voltage part of the characteristic when the device is optically active. If there is a sudden radial growth of a filament, this leads to a rapid conductivity increase and a short-circuit effect of the diode structure.

This can explain, at least partly, that sometimes in the highest-voltage region the current increases with the potential while EL is stable or decreases. Moreover, these effects also affect the lifetime of the sam-

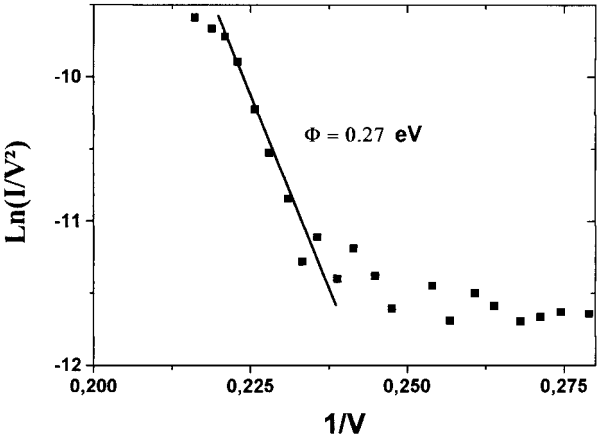

Figure 10 Fowler–Nordheim, $\ln(I/F^2) = (f)$, plot for SnO_2/CDV/Al (sample of Fig. 4).

ples. Since the NDR effect decreases when the film thickness increases, an optimum thickness value should be obtained to avoid the NDR effect without a too large EL efficiency decrease. An EL decrease with increase of the organic layer thickness is due to carrier trapping in the thick film before exciton formation. Moreover, the turn-on voltage increases with the film thickness and prohibitive values are rapidly measured.

As said before, the application of a reverse potential appears to be often more damaging than is the same forward bias. This fact can be explained by the filamentary model. In the presence of water, dissociated protons migrate much more easily than does hydroxyl because the mobility of the latter is smaller owing to its large ionic radius. Therefore, for a positive bias on the SnO_2 under the electrode, the protons migrate from the anode to the cathode upper layer. The proton source is limited to absorbed water and the filament will easily break when the proton source is exhausted.

In reverse polarization, protons migrate from the positive upper electrode toward negative SnO_2 under the electrode. In that case, the water present in air will be an additional proton source, which can justify the higher damages measured with reverse potential. Some authors showed that encapsulating the diodes increases their lifetime,[8] which is in good agreement with the model proposed above. After encapsulation, an extra proton source is suppressed and the lifetime should increase.

CONCLUSIONS

A polymer based on the thiophene vynilic derivative was electrochemically synthesized. It was shown that this polymer emits light between 600 and 720 nm. The structures SnO_2/CDV/Al based on this new polymer exhibit rectifying behavior. The forward direction corresponds to a SnO_2 electrode positively biased. Simultaneously, when the current is high enough, there is also light emission. The current in these structures is related to a Fowler–Nordheim tunneling effect.

The occurrence of an erratic but reversible NRD is explained by the roughness of the interfaces, which induces a high-field domain and localized conducting pathways with proton migration. Such conducting filaments can break and reform depending on the temperature. We interpreted the high sensitivity of the structure to reverse bias to these ionic conducting filaments, and we showed why encapsulation increases the lifetime. To increase the luminescence of the device structures based on CDV but with a second organic film, an electron-transporting layer will be deposited on the CDV layer before Al deposition.

The authors thank FONDECYT-CHILE and ECOS-CONICYT for financial support (Grants 8970011 and C99E05, respectively).

References

1. Burroughes, J. H.; Bradley, D. D. C.; Brown, A. R.; Marks, R. N.; Friend, R. H.; Burn, P. L.; Holmes, A. B. Nature 1990, 347, 539.
2. Halls, J. J. M.; Baigent, D. R.; Cacialli, F.; Greenham, N. C.; Friend, R. H.; Moratti, S. C.; Holmes, A. B. Thin Solid Films 1996, 276, 13.
3. Hosokana, C.; Higashi, H.; Nahamura, H.; Kusumoto, T. Appl Phys Lett 1995, 67, 3853.
4. Vestweber, H.; Rie, W. Synth Met B 1997, 91, 181.
5. Zhang, Z.-L.; Jiang, X.-Y.; Xu, S.-H.; Nagatomo, J.; Omoto, O. Synth Met 1997, 91, 131.
6. Jolnat, P.; Clergereaux, R.; Farenc, J.; Destruel, P. J Phys D Appl Phys 1998, 31, 1.
7. Miller, R.; Nord, R. J Org Chem 1951, 16, 1720.
8. Nguyen, T. P.; Molinié, P.; Destruel, P. In Handbook of Advanced Electronic and Photonic Materials and Devices; Nalwa, H. S., Ed.; Academic: San Diego, 2000.
9. Ostergrad, T.; Kvarnstrom, C.; Stubb, H.; Ivaska, A. Thin Solid Films 1997, 311, 58.
10. Damlin, P.; Ostergard, T.; Ivaska, A.; Stubb, H. Synth Met 1999, 102, 947.
11. Gordon, G. Mat Res Soc Symp Proc 1996, 426, 419.
12. Osada, T.; Kugler, Th.; Bröms, P.; Salaneck, W. S. Synth Met 1998, 96, 77.
13. Kern, W.; Puotinen, D. A. RCA Rev 1970, June, 187.
14. Messoussi, R. Thèse d'état, Kénitra, Maroc, 1998.
15. Córdova, R.; del Valle, M. A.; Gómez, H.; Schrebler, R. J Electroanal Chem 1994, 377, 75.
16. East, G. A.; del Valle, M. A. J Chem Ed 2000, 77, 97.
17. Shirley, A. Phys Rev B 1972, 5, 4709.
18. Beamson, G.; Briggs, D. High Resolution XPS of Organic Polymers; The Scienta ESCA 300 Database; Wiley: Chichester, 1992.
19. Kil, J. S.; Ho, P. K. H.; Thomas, D. S.; Friend, R. H.; Cocialli, F.; Bao, G. W.; Li, S. F. Y. Chem Phys Lett 1999, 315, 307.
20. Camplele, J.; Bradley, D. D. C.; Lawbender, J.; Sokolowski, M. J Appl Phys 1999, 86, 5004.
21. Sze, S. M. Physics of Semiconductor Devices; Wiley: New York, 1981; p 258.
22. Fowler, R. H.; Nordheim, L. Proc R Soc Lond Ser A 1928, 119, 173.
23. Taoudi, H.; Bernède, J. C.; Del Valle, M. A.; Bonnet, A.; Bonnet, A.; Molinié, P.; Morsli, M.; Diaz, F. J Appl Polym Sci 2000, 75, 1561.
24. Berleb, S.; Brütting, N.; Schaerer, M. Synth Met 1999, 102, 1034.
25. Ovshinsky, S. R. Phys Rev Lett 1968, 21, 1450.
26. Mott, N. F. Philos Mag 1975, 32, 159.
27. Hickmott, T. W. J Appl Phys 1964, 35, 2118.
28. Deamaley, G.; Stoneham, A. M.; Morgan, D. V. Rep Prog Phys 1970, 33, 1129.
29. Kimura, T.; Yamamoto, K.; Shimizy, T.; Yuga, S. Thin Solid Films 1980, 70, 351.